Geophysical Research Letters

RESEARCH LETTER
10.1029/2024GL110326

Reinterpreting ENSO's Role in Modulating Impactful Precipitation Events in California

Kristen Guirguis[1], Benjamin Hatchett[2], Alexander Gershunov[1], Michael DeFlorio[1], Rachel Clemesha[1], W. Tyler Brandt[1], Kayden Haleakala[1], Christopher Castellano[1], Rosa Luna Niño[1], Alexander Tardy[3], Michael Anderson[4], and F. Martin Ralph[1]

[1]Scripps Institution of Oceanography, University of California San Diego, La Jolla, CA, USA, [2]Cooperative Institute for Research in the Atmosphere, Colorado State University, Fort Collins, CO, USA, [3]US National Weather Service, San Diego, CA, USA, [4]California Department of Water Resources, Sacramento, CA, USA

Abstract Water years (WY) 2017 and 2023 were anomalously wet for California, each alleviating multiyear drought. In both cases, this was unexpected given La Niña conditions, with most seasonal forecasts favoring drier-than-normal winters. We analyze over seven decades of precipitation and snow records along with mid-tropospheric circulation to identify recurring weather patterns driving California precipitation and Sierra Nevada snowpack. Tropical forcing by ENSO causes subtle but important differences in these wet weather patterns, which largely drives the canonical seasonal ENSO-precipitation relationship. However, the seasonal frequency of these weather patterns is not strongly modulated by ENSO and remains a primary source of uncertainty for seasonal forecasting. Seasonal frequency of ENSO-independent weather patterns was a major cause of anomalous precipitation in WY2017, record-setting snow in WY2023, and differences in precipitation outcome during recent El Niño winters 1983, 1998, and 2016. Improved understanding of recurrent atmospheric weather patterns could help to improve seasonal precipitation forecasts.

Plain Language Summary In 2017 and 2023, California experienced unexpectedly wet conditions despite predictions of dry winters due to La Niña. In 2016, seasonal predictions in California favored wet conditions due to the very strong El Niño, but the season was normal-to-dry statewide. Understanding relationships between El Niño/La Niña and recurring atmospheric weather patterns driving individual storms is needed to improve seasonal forecasts. We studied historical relationships between weather patterns that bring rain and snow to the region and the El Niño Southern Oscillation (ENSO). We find ENSO influences important characteristics of weather patterns once they make landfall in California, making El Niño storms generally wetter in coastal southern California and Desert Southwest. However, ENSO does not strongly affect how often these patterns occur in a season, which makes seasonal precipitation forecasts challenging. The frequency of certain weather patterns not tied to ENSO played important roles in the unusual rainfall of 2017, the heavy snowfall of 2023, and the drier than expected winter of 2016. Understanding these weather patterns provides operationally and scientifically relevant context for future seasonal forecasts by highlighting that while ENSO only minimally influences the frequency of certain impactful storm types, it does change the precipitation characteristics of these storms.

Key Points:

- Weather regime type and frequency are key drivers of winter seasons with anomalous precipitation and/or snow accumulation in California
- ENSO does not modulate the seasonal frequency of weather regimes impacting the coast, presenting a challenge for seasonal forecasting
- ENSO modulates synoptic circulation characteristics of key weather regimes which produces the canonical ENSO-precipitation relationship

Supporting Information:

Supporting Information may be found in the online version of this article.

Correspondence to:

K. Guirguis,
kguirguis@ucsd.edu

Citation:

Guirguis, K., Hatchett, B., Gershunov, A., DeFlorio, M., Clemesha, R., Brandt, W. T., et al. (2024). Reinterpreting ENSO's role in modulating impactful precipitation events in California. *Geophysical Research Letters*, *51*, e2024GL110326. https://doi.org/10.1029/2024GL110326

Received 15 MAY 2024
Accepted 9 JUL 2024

1. Introduction

California winters bring volatile weather, often alternating between flood and drought, impacting residents, infrastructure, and the economy (Dettinger et al., 2011). This volatility challenges water resource managers in making decisions about water storage and flood/drought preparedness (DeFlorio et al., 2021). Seasonal precipitation predictions rely on observed relationships ("teleconnections") between precipitation and slowly varying climate modes, especially the El Niño-Southern Oscillation (ENSO). ENSO, a recurring climate mode, affects ocean heat content in the tropical Pacific. La Niña (El Niño) is associated with cooler (warmer) waters in the eastern tropical Pacific along with weaker (stronger) easterly trade winds, which through tropical convection and atmospheric teleconnections can affect global temperature and regional weather and extremes (Bjerknes, 1966; Diaz & Markgraf, 2000; Goddard & Gershunov, 2020; Hoerling et al., 1997; Horel & Wallace, 1981; Rasmusson & Wallace, 1983). In the North Pacific, El Niño is associated with an extension and equatorward shift of the East Asian polar jet, a deepening of the Aleutian Low, and changes in upper-level atmospheric circulation over western North America (Hoerling et al., 1997; Horel & Wallace, 1981). In a composite

sense, El Niño alters the pattern of Pacific Rossby waves by fostering negative (positive) geopotential height anomalies over the North Pacific Ocean (western Canada) whereas La Niña brings an opposite pattern (Figure S1a in Supporting Information S1; Hoerling et al., 1997). In southern California and the Desert Southwest, El Niño (La Niña) is often associated wetter (drier) conditions; with the inverse observed in the Pacific Northwest (Figure S1b in Supporting Information S1; Cayan et al., 1999; Redmond & Koch, 1991).

The ENSO-precipitation teleconnection is considered an important source of California hydroclimate predictability (e.g., Gershunov, 1998; Goddard et al., 2003; Patricola et al., 2020). However, recent years have brought important deviations from the canonical ENSO-precipitation relationship, and as a result, seasonal forecasts have not been skillful in California. For example, the La Niña winter of 2011 was exceptionally wet. After 4 years of severe drought that followed, the very strong ("Godzilla") El Niño winter 2016 was expected to be exceptionally wet (on par with 1983 and 1998 based on sea surface temperature anomalies). However, this did not manifest and 2016 was instead normal-to-dry in most of the State (Kintisch, 2016). The following winter in 2017, a weak La Niña, brought one of the wettest years on record due to repeated atmospheric river (AR) landfalls that officially ended 4 years of drought. However, WY2017 also caused extensive and costly flooding (California Department of Water Resources, 2017). The winter of 2023 broke many precipitation-related records, especially snowfall, which defied seasonal predictions based on La Niña conditions (DeFlorio et al., 2023). Some research has identified internal atmospheric variability as the cause of recent unexpected outcomes (Cash & Burls, 2019; Dong et al., 2018; Jiang et al., 2022; Kumar & Chen, 2017; Zhang et al., 2018). Other research highlights the role of "ENSO diversity" or nonlinearity in the ENSO response (e.g., Patricola et al., 2020).

Most of California's winter precipitation is delivered by reoccurring atmospheric weather patterns characterized by an upper-level trough over or upstream of California, which results in enhanced moisture transport over the coast and mountain topography. Certain configurations of trough position, orientation, and resulting pressure gradient, have been linked to atmospheric rivers, extreme precipitation, and flooding (e.g., Fish et al., 2019; Guirguis et al., 2023a; Neiman et al., 2008; Weaver, 1962). In this study, we examine relationships between the seasonal ENSO state and these recurring wet weather patterns to explain climate-weather linkages important for seasonal predictability. We use a previously published historical catalog of observed winter atmospheric weather regimes, along with precipitation and snow records to first identify weather patterns associated with statewide precipitation and Sierra Nevada snowpack. We then examine if/how ENSO modulates the frequency or other characteristics of these influential weather patterns to highlight important relationships between daily weather systems and the more slowly evolving background climate state. In this context, we then examine recent winters of interest for their poor seasonal forecast outcomes (WY2016, WY2017, and WY2023).

2. Data and Methods

2.1. Atmospheric Circulation

We use 500 mb geopotential height (Z500) and wind from NCEP/NCAR global reanalysis (R1, Kalnay et al., 1996) available from 1948, with anomalies calculated by fitting and removing annual/semi-annual seasonal cycles.

2.2. Daily Atmospheric Weather Patterns

Atmospheric weather "patterns" (interchangeably referred to as "regimes") are from Guirguis et al. (2023a, 2023b), hereinafter GGR'23, extended to October–March 1948–2023. This provides a daily record of observed Z500 anomaly patterns over the northern Pacific Ocean and western US. Each day is classified as 1 of 16 recurring weather patterns, which have been previously validated for representing observed atmospheric circulation, and for their associated impacts over California and the western US including for precipitation, atmospheric rivers, and historic California floods; as well as for Santa Ana winds in Southern California (GGR'23) and California mid-winter drought (Hatchett et al., 2023). The 16 weather regimes representing recurring atmospheric circulation patterns are shown in Figure S2 of the Supporting Information S1, along with corresponding precipitation and temperature anomalies. The subset of weather regimes associated with California precipitation all feature a trough over/offshore California, and bear similarity to weather patterns identified in other studies of impactful winter storms using different methods (e.g., hydrologically critical storms of Weaver (1962); atmospheric river families of Fish et al. (2019)). Additional details about the weather regime defining methodology are provided in Text S1 and Figure S3 in Supporting Information S1.

2.3. Precipitation and Temperature

Precipitation and daily maximum temperature (Tmax) are from gridMET (Abatzoglou, 2013) available from 1979 at a spatial resolution of 4 km.

2.4. Snowfall

To estimate snow fraction over the Sierra Nevada we calculate the proportion of precipitation occurring when daily Tmax was below 3°C (Shulgina et al., 2023). We also use in situ daily snowfall data from two high-quality National Weather Service (NWS) Cooperative Observer Program (COOP) stations located at different elevations and latitudes in the Sierra Nevada. These are Tahoe City (39.14°N, 120.18°W, elevation 1,899 m/6,230 feet) in the Northern Sierra Nevada, just east of the Sierra Nevada crest, and Hetch Hetchy (37.96°N, 119.78°W, elevation 1,179.6 m/3,870 feet) along the western slope in the Central Sierra Nevada (Figure 1b). These stations were chosen for their geographic relevance and comprehensive records (<3% missing). The records used span 1950-present and include daily precipitation and snowfall measurements.

2.5. Atmospheric River Landfalls and Intensity Scale

We employ the SIO-R1 catalog (Gershunov et al., 2017) to identify landfalling ARs based on specific criteria for vertically integrated vapor transport (IVT) and vertically integrated water vapor (IWV) from R1, alongside geometric length/width requirements. ARs are categorized using the 5-scale system of Ralph et al. (2019), with scales 1–2 indicating lower hazard and scales 4–5 indicating higher hazard with peak IVT ranging from 750 to >1,250 kg m^{-1} s^{-1}.

2.6. ENSO

We utilize Nino3.4 (sea surface temperatures averaged over 5°S–5°N and 170°–120°W) from the Climate Prediction Center. El Niño (La Niña) winters are identified when October-March Niño3.4 averages deviate above (below) 0.5 standard deviations from the mean. We also use the ENSO Longitude Index (ELI, Patricola et al., 2020) to measure ENSO diversity by the longitude of tropical Pacific deep convection, extended through 2023.

3. Weather Regimes Important for Precipitation, Atmospheric Rivers, and Sierra Nevada Snowpack

The recurring atmospheric weather patterns identified in GGR'23, along with their associated precipitation and temperature anomaly patterns, are shown in Figure S2 in Supporting Information S1. The subset of weather regimes responsible for most of California's statewide precipitation and Sierra Nevada snowpack (weather regimes 8–14, the "wet weather regimes") are the focus of this study. Note that although WR13 presents as drier than average in California, precipitation does occur during this regime and, because it is also very cold, WR13 is important for snow in the Sierra Nevada.

The weather regimes responsible for delivering most of California's precipitation (WR8-14) are displayed seperately in Figure 1a. They are all characterized by a trough positioned favorably for anomalous moist onshore flow over California. The spatial variability and magnitude of precipitation depends on the position and orientation of the trough relative to California's coastline and mountain topography (O'Hara et al., 2009; Hatchett et al., 2017; GGR'23). Some patterns (WR8-10) are more impactful for northern/central California, and others (WR11-14) impact southern California more. The coldest patterns (WR11-14) feature a very deep trough extending over most of California, favoring cold air advection into the region. This combination of cold air advection and moist onshore flow is important for snow. Collectively, these "wet weather regimes" account for up to 80% of total historical precipitation in California (Figure 1b), and they are especially important for precipitation and snowfall in the Sierra Nevada range, where snowpack forms a key natural reservoir.

While all these wet weather patterns are important for California precipitation, there are important distinctions among them. The capacity for moisture transport is greatest for WR8-10 (Figure S4a in Supporting

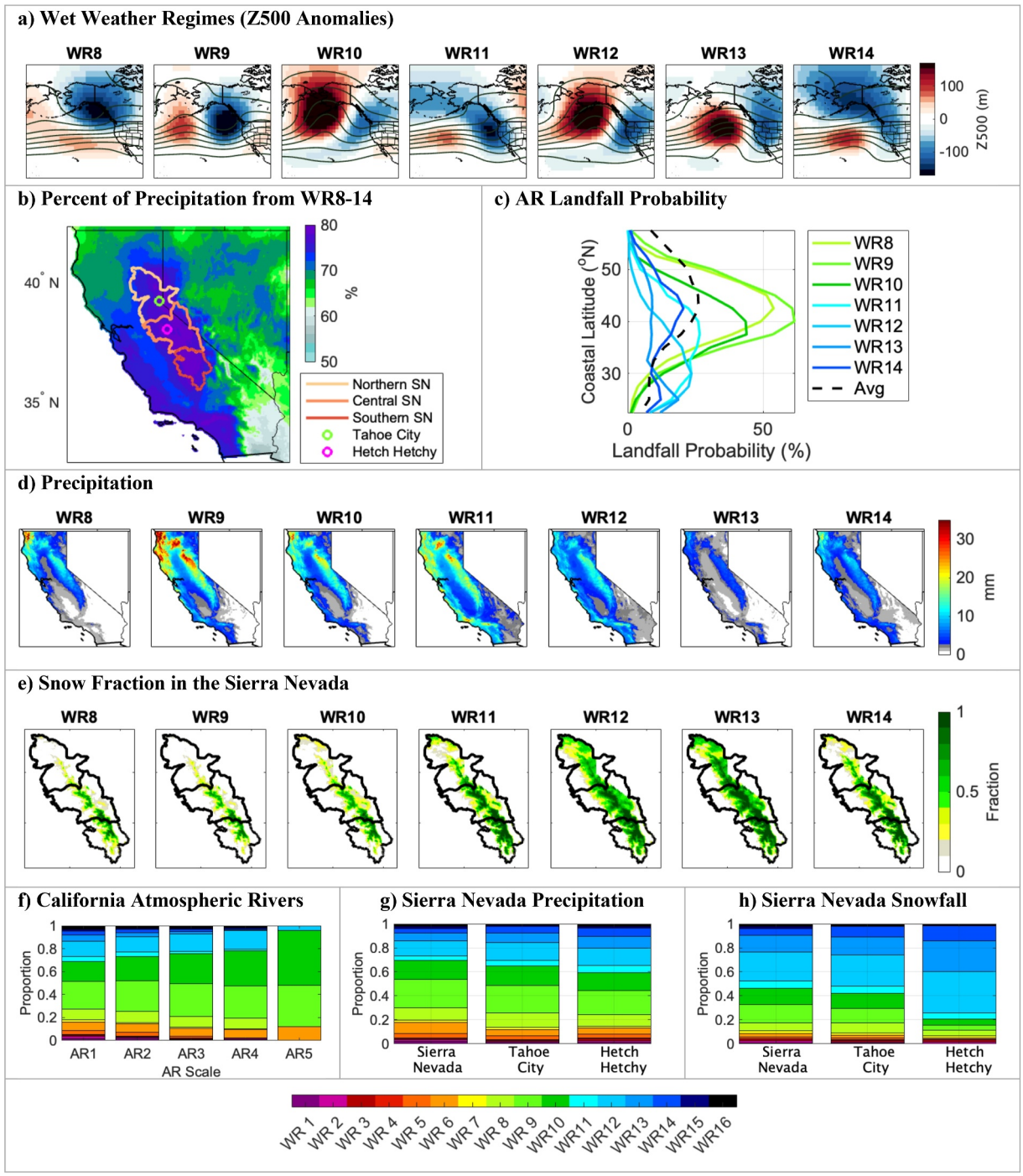

Figure 1. (a) The wet weather regimes shown as Z500 anomalies. (b) Percent of historical (1979–2023) precipitation that fell during WR8-14 with outlines of the Northern, Central, and Southern Sierra Nevada and locations of Tahoe City and Hetch Hetchy Coop stations. (c) AR landfall probability at different coastal latitudes for WR8-14. (d) Average daily precipitation from WR8-14. (e) Snow fraction over the Sierra Nevada for WR8-14. (f) Proportion of California ARs of different categories for each weather regime using the AR scale of Ralph et al. (2019). (g and h) Weather regime contribution to (g) precipitation and (h) snowfall in the Sierra Nevada displayed as proportion of the historical total.

Information S1), and these types of weather patterns are more likely to cause California AR landfalls (Figure 1c, green lines). Two weather patterns, WR9-10, are largely responsible for the strongest and potentially hazardous AR storms representing 59% and 84% of AR scale 4 and 5 storms, respectively (Figure 1f).

The other wet weather pattens, WR11-14, are not quite as efficient at transporting moisture, but they yield colder storms, so the Pacific moisture transported to California is more likely to be mixed with very cold air, lowering snow levels and increasing snow-liquid ratios. We can see how the circulation field enhances these favorable conditions for snow by comparing 700 mb temperature fields (Figure S4b in Supporting Information S1). Weather regimes 8–10 are associated with average temperatures over California with anomalous cold air located to the north or northeast. In contrast, WR11-14 are characterized by a deep trough driving cold air advection into California, which is seen by the cold temperature anomaly positioned directly over California. It follows that WR11-14 (and especially WR12-13) produce higher snow fractions over the Sierra Nevada (Figure 1e) while contributing less to overall California precipitation (Figure 1d).

In terms of Sierra Nevada water accumulation, the wet weather regimes collectively account for 76% of total historical precipitation (Figure 1g, blue and green shading combined) and 85% of snowfall (Figure 1h, blue and green shading combined). The warmer wet weather regimes (WR8-10) collectively make up a larger proportion of precipitation (Figure 1g, green shading), whereas the colder wet weather patterns (WR11-14) collectively make up a larger proportion of snow (Figure 1h, blue shading). The importance of the cold wet weather patterns for snowfall is especially notable at lower elevations as represented by Hetch Hetchy (Figure 1h, blue shading).

Since these wet weather patterns are responsible for delivering most of California's precipitation and Sierra Nevada snowpack, understanding relationships with ENSO is important for seasonal predictability.

4. Modulation by ENSO

Having identified weather regimes for their impacts in California, we now investigate if/how ENSO influences these weather regimes in a way that explains the observed canonical ENSO-precipitation signal. The canonical relationship between ENSO and precipitation, extensively explored in previous studies (e.g., Cayan et al., 1999; DeFlorio et al., 2013; Gershunov, 1998; Hoell et al., 2016; Redmond & Koch, 1991), is depicted in Figure S1b of the Supporting Information S1. El Niño is generally associated with somewhat drier-than-normal conditions in the Pacific Northwest and wetter-than-normal conditions in California and the Southwest, particularly in the Sonoran and Mojave deserts where relatively small precipitation events can produce a large anomaly relative to climatology. The inverse pattern is largely observed during La Niña.

4.1. Weather Regime Frequency

Seasonal weather regime frequency (i.e., how often each weather regime occurs in a season) explains the majority of interannual precipitation variance over most locations in the Western US (Figure S5 in Supporting Information S1). Therefore, one consideration tested in this study is whether ENSO modulates the seasonal frequency of wet weather patterns in a way that explains the canonical ENSO-precipitation teleconnection pattern. The seasonal frequency of each weather regime is shown in Figure 2a for different phases of ENSO using Nino3.4. Some differences are apparent; however, these differences are small, lack consistency, and do not explain the canonical ENSO-precipitation teleconnection. The strongest frequency differences are observed for WR6 and WR13, where WR6 (WR13) occurs more frequently during El Niño (La Niña). However, WR6 typically brings more (less) precipitation to the Pacific Northwest (Southern California and Desert Southwest) relative to WR13, which is counter to the canonical ENSO-precipitation relationship (Figure S6 in Supporting Information S1). Importantly, there are only minor differences in frequency for WR9 and WR10, which are the wettest weather regimes associated with California extreme ARs and historic floods, or for WR12, which is the regime that makes the largest contribution to low-to-mid-elevation Sierra Nevada snow. We also performed this analysis using the ELI to account for ENSO diversity with similar results (Figure S7 in Supporting Information S1).

To provide event-level examples, Figures S8 and S9 in Supporting Information S1 show atmospheric circulation patterns for historical cases when the wettest regimes WR9 or WR10 occurred on five or more consecutive days, respectively. Many impactful California floods are identified; and they occurred across ENSO states (color-coded in the title). The corresponding IVT fields are shown in Figures S10 and S11 of the Supporting Information S1, respectively, highlighting AR conditions brought by these persistent weather patterns. For example, the New Year's Day Flood of 1997 (Figures S8 and S10 in Supporting Information S1) and the February 2017 Oroville Dam Crisis (Figures S9 and S11 in Supporting Information S1) are included, both of which brought substantial

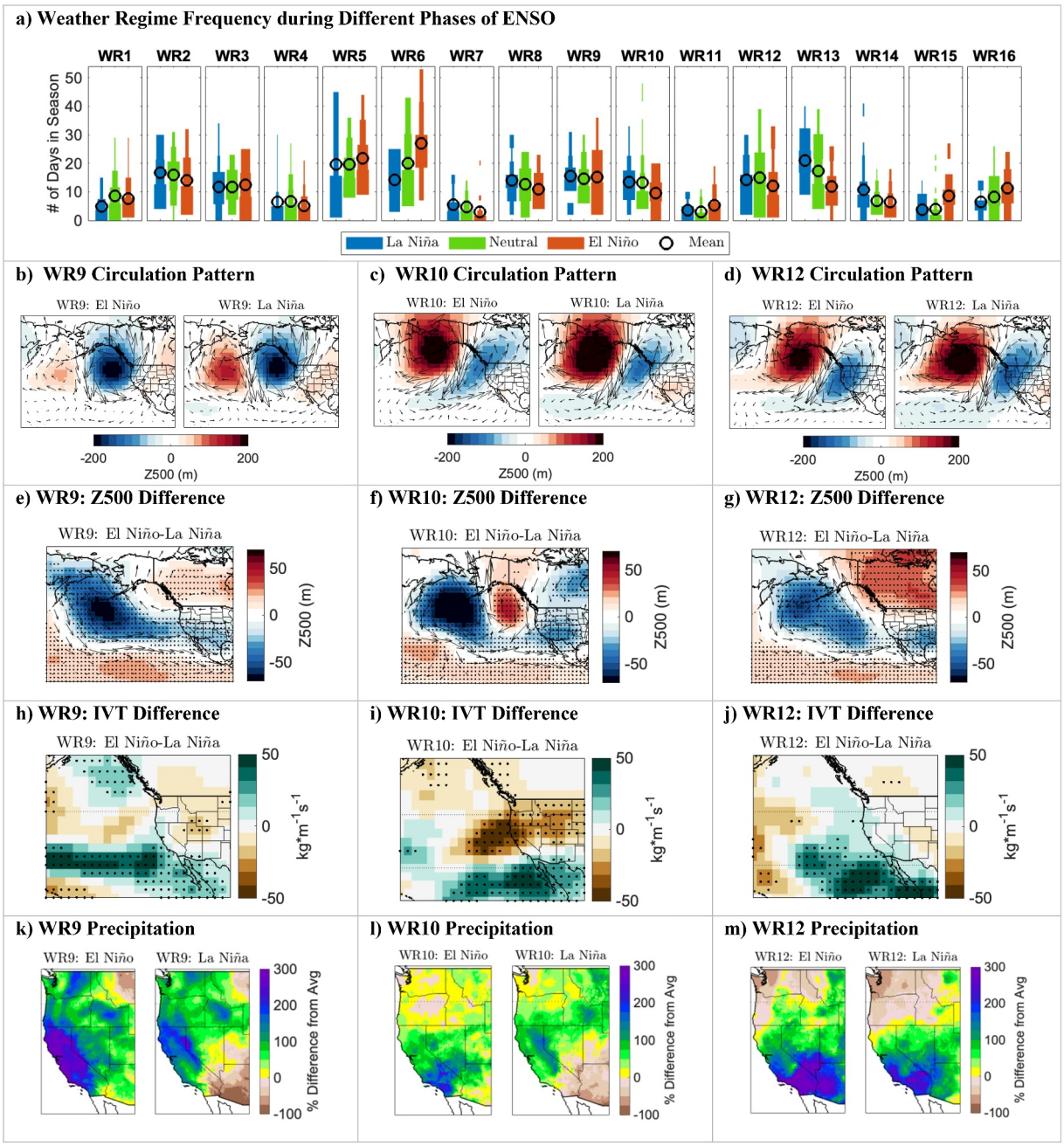

Figure 2. (a) Seasonal weather regime frequency (*y*-axis) conditional on ENSO phase (color scale), shown as a hybrid of a boxplot and histogram where the bar width represents the proportion of data in a bin and the "o" denotes the mean. (b–d) Z500 anomaly patterns for WR9, WR10, and WR12 during El Niño (left) and La Niña (right). (e–g) Difference in Z500 fields shown as El Niño minus La Niña (h–j) Difference in IVT shown as El Niño minus La Niña for WR9, WR10, and WR12. (k–m) Precipitation anomalies for WR9, WR10, WR12 during El Niño (left) and La Niña (right). Stippling in (e)–(g) and (h)–(j) indicates statistically significant differences (5% level, student's *t*-test).

storm-total precipitation and high elevation rain-on-snow (Haleakala et al., 2023; Rhoades et al., 2023) and occurred during a weak La Niña.

These results highlight the recurrent nature of impactful weather patterns and reveal that ENSO does not significantly modulate their seasonal frequency in a manner consistent with the canonical ENSO-precipitation signals. This helps support earlier studies showing a lack of ENSO impact on AR landfall frequencies along the west coast (Gershunov et al., 2017; Guan & Waliser, 2015; Guirguis et al., 2019).

4.2. Weather Regime Circulation and Ridge/Trough Amplification

We now consider whether and how ENSO modulates circulation characteristics of the wet weather regimes, focusing first on the regimes most important for extreme ARs (WR9 and WR10) and Sierra Nevada snowpack (WR12). The atmospheric circulation patterns for each of these regimes under different ENSO states is shown in Figures 2b–2d. They are highly similar during La Niña and El Niño. However, there are some important differences. For example, for WR9 (Figure 2b), the atmospheric circulation patterns during La Niña and El Niño are nearly indistinguishable (spatial anomaly correlation = 0.91) with both patterns featuring a deep trough in the Gulf of Alaska and an upstream ridge over the western Pacific and a downstream ridge over Baja California that extends over the central/eastern US. However, the ridging is amplified during La Niña (right) and reduced during El Niño (left). This amplified ridge during La Niña is characteristic of the known ENSO-Z500 teleconnection pattern (cf. Figure S1a in Supporting Information S1). The analysis for WR10 and WR12 shows similar ridge amplification (reduction) during La Niña (El Niño) while otherwise the patterns are very similar (Figures 2c and 2d). Also notable is the enhanced ridge over Baja California during La Niña, relative to El Niño, which modifies the storm track over California. Overall, these subtle modifications by ENSO allow the Pacific trough to extend equatorward and closer to shore during El Niño relative to La Niña, enhancing flow over Southern California (Figures 2e–2g, shown as El Niño minus La Niña).

The IVT fields associated with these weather regimes under different ENSO states highlights a southward displacement of the storm track during El Niño relative to La Niña (Figures 2h–2j). This displacement affects the precipitation outcomes over California (Figures 2k–2m). Regardless of the ENSO state, these weather patterns bring anomalously wet conditions to California. However, during El Niño, storms brought by these weather regimes tend to be wetter, on average, than during La Niña, especially over coastal Southern California and the Desert Southwest.

The circulation composites for all the wet weather regimes are shown in Figure S12 of the Supporting Information S1. Visually, the El Niño and La Niña patterns are nearly indistinguishable. However, the difference maps (Figure S12c in Supporting Information S1) show that, relative to La Niña, El Niño is associated with negative Z500 anomalies over the Pacific with enhanced westerly flow extended at California latitudes. The average across all weather regimes (Figure S12d in Supporting Information S1) shows strong similarity to the known ENSO-Z500 teleconnection pattern shown in Figure S1c of the Supporting Information S1 ($r = 0.89$, spatial correlation). This demonstrates how weather-scale variability (i.e., the weather regimes) occurs on top of the background ENSO state.

ENSO does not directly initiate or alter the likelihood of wet weather patterns, but it does impact circulation, typically resulting in wetter storms during El Niño in the coastal ranges and valleys of California and the Desert Southwest. Precipitation anomalies for all the wet weather regimes during different phases of ENSO are shown in Figures S13a and S13b of the Supporting Information S1, with differences illustrated in Figure S13c of the Supporting Information S1. Wet conditions are observed regardless of ENSO state, yet El Niño consistently enhances precipitation, relative to La Niña, particularly in the southern and western regions (Coast, Transverse, and Peninsular Ranges). The average ENSO signal across weather regimes aligns closely with the known canonical ENSO-precipitation teleconnection pattern (i.e., compare Figure S13d with Figure S1d of the Supporting Information S1 (spatial correlation = 0.98)). This reveals how ENSO influences western US precipitation primarily through modulating transient ENSO-independent weather patterns.

5. Recent Winters

5.1. El Niño Winters of 1983, 1998, and 2016

Considering the relatively dry California winter of 2016 compared to the wetter El Niño winters of 1983 and 1998, we explore how seasonal weather regime frequency disrupts the canonical ENSO-precipitation teleconnection pattern over California. The frequency of the wet weather regimes differed among these El Niño winters (Figure 3a), with notably fewer days in 2016 (55 days) compared to 1983 (88 days) and 1998 (86 days). These wet weather regimes contributed significantly to seasonal precipitation, accounting for up to 88% and 76% of seasonal precipitation in WY1983 and WY1998, respectively (Figure S14 in Supporting Information S1).

During the two very wet seasons, WR9 played a crucial role, accounting for a substantial proportion of precipitation statewide (38% in 1983 and 23% in 1998) and in the Sierra Nevada (42% in 1983 and 23% in 1998).

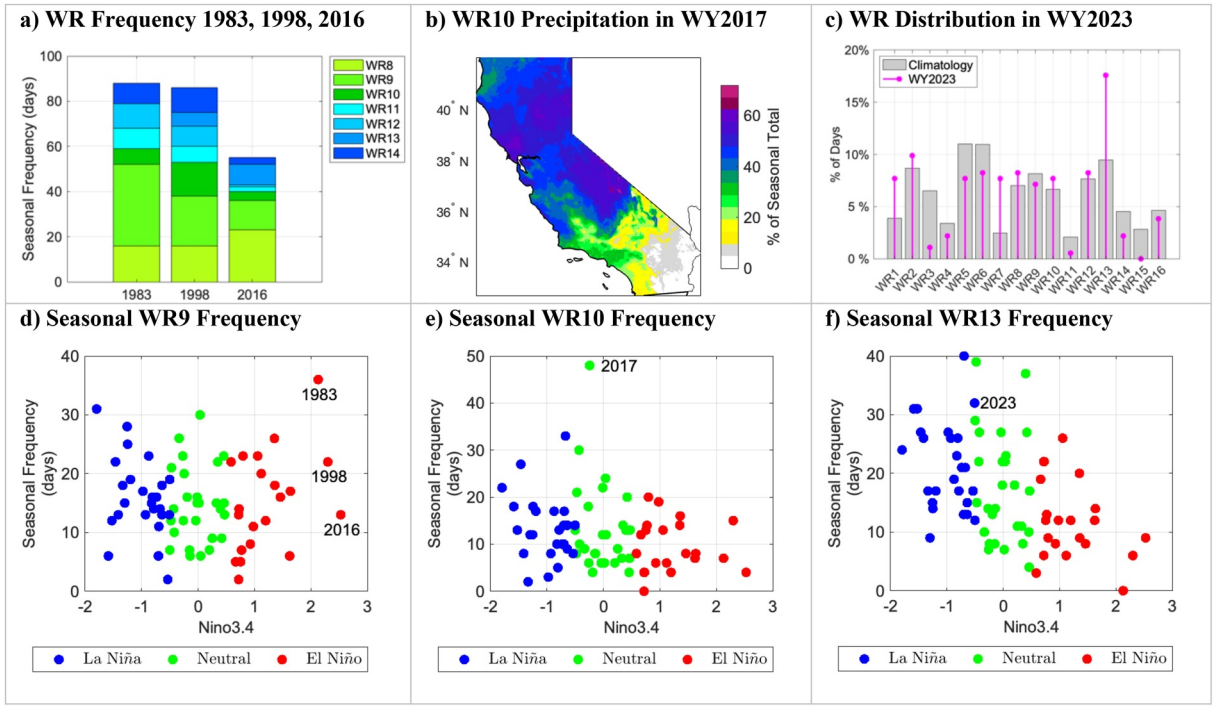

Figure 3. (a) Seasonal frequency of the wet weather regimes during WY1983, WY1998, and WY2016. (b) Amount of precipitation that fell during WY2017 on days classified as WR10, shown as % of seasonal total. (c) Weather regime frequency over the historical period (climatology, gray) and during WY2023 (pink) expressed as the percentage of days in the season. (d–f) Relationship between ENSO and the seasonal frequency of WR9, WR10, and WR13 highlighting recent years of poor seasonal forecasts.

Historically, this weather pattern is among the wettest for California and is linked to extreme ARs (cf. Figure 1f) and historic California floods (GGR'23).

There is no observed relationship between WR9 frequency and ENSO (Figure 3d, $r^2 \approx 0$). WR9 occurred less frequently in WY2016 (13 days, or about 2 days below average) compared to WY1983 (36 days) or WY1998 (22 days). The high frequency of WR9 during 1983 was anomalous, suggesting that the exceptionally wet conditions that year were likely due to a combination of weather-scale variability (elevated frequency of WR9) and El Niño's influence on the storm track (cf., Figure 2). For reference, in 1983 this highly prevalent weather pattern brought approximately 74% of the total amount of precipitation received in the Sierra Nevada in a typical season. Sensitivity tests using ELI to test the role of ENSO diversity are shown in Figure S15 of the Supporting Information S1, which does not improve the relationship ($r^2 = 0.02$, $p > 0.1$). It's noteworthy that WR10, another pattern linked to extreme ARs, was also more frequent in WY1983 (7 days) and WY1998 (15 days) than in WY2016 (4 days, Figure 3a).

5.2. Winter of 2017

WY2017 was unusually wet, with the most active atmospheric river season in California using records going back to 1948 (Gershunov et al., 2017). This was unexpected because it occurred during what is often considered a weak La Niña (classified as neutral by our criteria). The prevalence of WR10 during that winter was highly anomalous, occurring on 48 days (30 more days than occurs on average, Figure 3e). WR10 accounted for over half of seasonal precipitation in parts of coastal Northern California and the Sierra Nevada (Figure 3b), including the extreme precipitation event from February 1–8, which caused severe flooding and damage to the Oroville Dam spillway. This damage resulted not only from heavy precipitation but also from very high runoff due to saturated soils from previous storms (also WR10; Haleakala et al., 2023; Michaelis et al., 2022; Siirila-Woodburn et al., 2023). These repeated long-duration WR10 storms during WY2017 are seen in Figures S9 (Z500) and S11 (IVT) of the Supporting Information S1. The frequency of WR10 (Figure 3e) is not significantly influenced by ENSO ($r^2 = 0.07$, $p > 0.02$ using Niño3.4; $r^2 = 0.04$, $p > 0.1$ using ELI) suggesting these weather patterns occur with similar frequency in La Niña, El Niño, and ENSO-neutral years.

5.3. Winter of 2023

The weather regime frequency during WY2023 is shown in Figure 3c. In general, most of the wet weather patterns occurred with average or slightly above-average frequency, except for WR13, which occurred on 32 days, or 17.6% of the season (climatology = 9.5%). WR13, which is characterized by a deep trough over the western US (cf., Figure 1a), brought very cold conditions to California that year. In WY2023, WR13 was the largest contributor to snowfall, accounting for 26% overall in the Sierra Nevada, 33% at mid-elevation Tahoe City, and 48% at low-elevation Hetch Hetchy (Figure S16 in Supporting Information S1). The two wettest periods were December 26–January 17 and February 22–March 7. The December–January event brought a series of ARs to California (DeFlorio et al., 2023) and was responsible for about 40% of seasonal total precipitation in the Sierra Nevada. The February–March event brought less precipitation overall but was responsible for much of the season's snow (27% at Tahoe and 56% at Hetch Hetchy), including rare blizzard conditions at low elevations (Leanard, 2023). The December 26–January 17 AR sequence featured warmer variety wet weather patterns with a Pacific trough offshore (Figure S17 in Supporting Information S1, left) while the second, snowier accumulation period during February 22–March 7 was dominated by colder weather patterns with a deep trough positioned over the western US and California (Figure S17 in Supporting Information S1, right).

The high occurrence of WR13 during WY2023 explains the record-setting snow, particularly at low elevations. There is a significant linear relationship between WR13 frequency and ENSO (Figure 3f), with a higher frequency during La Niña ($r^2 = 0.22$, $p < 0.001$ using Niño3.4; $r^2 = 0.16$, $p < 0.001$ using ELI). However, the 32-day occurrence of WR13 during WY2023 is at the high end of the historical distribution, even considering La Niña conditions (5th highest seasonal frequency on record spanning 1948–2023).

6. Discussion

In this study, we identified key atmospheric weather regimes that deliver most of California's precipitation and Sierra Nevada snowpack. These regimes all feature a trough over or upstream of California, facilitating onshore moisture transport from the Pacific, and are similar in spatial structure to those identified in earlier studies of impactful winter storms (e.g., Fish et al., 2019; Weaver, 1962). Interannually, the frequency of these hydrologically critical weather regimes (Weaver, 1962) varies with consequences for California water resources. Our findings suggest that ENSO only minimally impacts the frequency of these wet weather patterns, adding uncertainty to seasonal forecasts. However, ENSO does influence other regime characteristics. El Niño storms typically feature enhanced westerly flow and an equatorward-shifted storm track relative to La Niña storms during otherwise very similar synoptic conditions, aligning with previous studies (e.g., Guirguis et al., 2019; Hu et al., 2017). This results in wetter storms in California during El Niño, especially in the south, which largely explains the canonical ENSO-precipitation teleconnection over the West. In our interpretation, the wet weather patterns are manifestations of high-frequency internal atmospheric variability, and the precipitation resulting from these weather patterns can be amplified or suppressed by the ENSO teleconnection pattern, which varies on longer timescales and thus modulates the background state.

We examined recent winters of interest for their poor seasonal forecast outcomes (WY2016, WY2017, and WY2023) and found weather regime frequency to be an important contributor. WY2016 had many fewer days with precipitation-producing weather patterns compared to WY1983 and WY1998, explaining its dryness despite being a strong El Niño year. Additionally, 1983 was identified as an outlier for its exceptionally high frequency of a particularly wet and ENSO-independent weather pattern (WR9), which suggests perhaps El Niño is given too much credit for the extremely wet conditions observed in that year (and which could bias seasonal forecasts based on historical El Niño-precipitation relationships). WY2017 was notable for its highly anomalous frequency of another high-impact weather pattern (WR10), contributing to the Oroville Dam crisis. WY2023's snowy conditions were linked to the high frequency of a cold advection-favoring weather pattern (WR13), which was the largest contributor to Sierra Nevada snowfall that season.

These results have implications for seasonal forecasting. While the canonical ENSO-precipitation relationship remains a key predictor, ENSO does not control the frequency of impactful weather patterns leaving much interannual variability unexplained. Our results suggest neither ENSO magnitude nor diversity explains interannual variations in weather regime frequency, suggesting recent forecast errors may stem from internal atmospheric variability independent of ENSO (e.g., Dong et al., 2018; Jiang et al., 2022).

SST variations beyond the tropical Pacific and interactions between other climate drivers (e.g., Pacific Decadal Oscillation, Madden Julian Oscillation, tropical/Northern Hemisphere pattern, etc.) are known to be important for modulating precipitation in the West (e.g., Gershunov & Barnett, 1998; Liu et al., 2018; Paek et al., 2017; Wang et al., 2024). Understanding how ENSO and other climate modes influence high-impact weather regimes could enhance management efforts, as weather regimes demonstrate some predictability at subseasonal timescales (Guirguis et al., 2023c). This research aims to inform improved predictability to prepare for upcoming events and communicate relevant information about how certain storms may differ from normal.

Data Availability Statement

The historical winter weather regime catalog is from Guirguis et al. (2023a, 2023b). The SIO-R1 AR catalog is from Gershunov et al. (2017). The gridMET temperature and precipitation data sets are from Abatzoglou (2013). The NCEP/NCAR reanalysis is from Kalnay et al. (1996). The COOP station data is from National Weather Service (2024).

Acknowledgments
This research was funded by the CW3E Atmospheric River Program, the California Department of Water Resources (600010378 UCOP2-11) and contributes to DOI's Southwest Climate Adaptation Science Center which is managed by the USGS National Climate Adaptation Science Center (G18AC00320). An extension to the 1950–2020 ENSO Longitudinal Index values from Patricola et al. (2020) for the period spanning 2021–2023 was kindly provided by John P. O'Brien. We thank two anonymous reviewers for their thoughtful and helpful feedback during this review process.

References

Abatzoglou, J. T. (2013). Development of gridded surface meteorological data for ecological applications and modelling. [Dataset]. *International Journal of Climatology*, *33*(1), 121–131. https://doi.org/10.1002/joc.3413

Bjerknes, J. (1966). A possible response of the atmospheric Hadley circulation to equatorial anomalies of ocean temperature. *Tellus*, *18*(4), 820–829. https://doi.org/10.1111/j.2153-3490.1966.tb00303.x

California Department of Water Resources. (2017). Water year 2017: What a difference a year makes. Retrieved from https://cawaterlibrary.net/document/water-year-2017-what-a-difference-a-year-makes

Cash, B. A., & Burls, N. J. (2019). Predictable and unpredictable aspects of U.S. West Coast rainfall and El Niño: Understanding the 2015/16 event. *Journal of Climate*, *32*(10), 2843–2868. https://doi.org/10.1175/JCLI-D-18-0181.1

Cayan, D. R., Redmond, K. T., & Riddle, L. G. (1999). ENSO and hydrologic extremes in the western United States. *Journal of Climate*, *12*(9), 2881–2893. https://doi.org/10.1175/1520-0442(1999)012<2881:eaheit>2.0.co;2

DeFlorio, M. J., Sengupta, A., Castellano, C. M., Wang, J., Zhang, Z., Gershunov, A., et al. (2023). From California's extreme drought to major flooding: Evaluating and synthesizing experimental seasonal and subseasonal forecasts of landfalling atmospheric rivers and extreme precipitation during winter 2022–2023. *Bulletin America Meteorology Social*. https://doi.org/10.1175/BAMS-D-22-0208.1

DeFlorio, M. J., Pierce, D. W., Cayan, D. R., & Miller, A. J. (2013). Western U.S. extreme precipitation events and their relation to ENSO and PDO in CCSM4. *Journal of Climate*, *26*(12), 4231–4243. https://doi.org/10.1175/JCLI-D-12-00257.1

DeFlorio, M. J., Ralph, F. M., Waliser, D. E., Jones, J., & Anderson, M. L. (2021). Better subseasonal-to-seasonal forecasts for water management. *Eos*, *102*. https://doi.org/10.1029/2021EO159749

Dettinger, M. D., Ralph, F. M., Das, T., Neiman, P. J., & Cayan, D. (2011). Atmospheric rivers, foods and the water resources of California. *Water*, *3*(2), 445–478. https://doi.org/10.3390/w3020445

H. F. Diaz, & V. Markgraf (Eds.) (2000). *El Niño and the southern oscillation: Multiscale variability and global and regional impacts*. Cambridge University Press.

Dong, L., Leung, L. R., Song, F., & Lu, J. (2018). Roles of SST versus internal atmospheric variability in winter extreme precipitation variability along the U.S. West Coast. *Journal of Climate*, *31*(19), 8039–8058. https://doi.org/10.1175/JCLI-D-18-0062.1

Fish, M. A., Wilson, A. M., & Ralph, F. M. (2019). Atmospheric river families: Definition and associated synoptic conditions. *Journal of Hydrometeorology*, *20*(10), 2091–2108. https://doi.org/10.1175/JHM-D-18-0217.1

Gershunov, A. (1998). ENSO influence on intraseasonal extreme rainfall and temperature frequencies in the contiguous US: Implications for long-range predictability. *Journal of Climate*, *11*(12), 3192–3203. https://doi.org/10.1175/1520-0442(1998)011<3192:eioier>2.0.co;2

Gershunov, A., & Barnett, T. P. (1998). Interdecadal modulation of ENSO teleconnections. *Bulletin of the American Meteorological Society*, *79*(12), 2715–2725. https://doi.org/10.1175/1520-0477(1998)079<2715:imoet>2.0.co;2

Gershunov, A., Shulgina, T., Ralph, F. M., Lavers, F., & Rutz, J. J. (2017). Assessing the climate-scale variability of Atmospheric Rivers affecting the west coast of North America [Dataset]. *Geophysical Research Letters*, *44*(15), 7900–7908. https://doi.org/10.1002/2017gl074175

Goddard, L., Barnston, A. G., & Mason, S. J. (2003). Evaluation of the IRI'S "Net Assessment" seasonal climate forecasts: 1997–2001. *Bulletin America Meteorology Social*, *84*(12), 1761–1782. https://doi.org/10.1175/BAMS-84-12-1761

Goddard, L., & Gershunov, A. (2020). Impact of El Niño on weather and climate extremes. In M. J. McPhaden, A. Santoso, & W. Cai (Eds.), *El Niño southern oscillation in a changing climate*. https://doi.org/10.1002/9781119548164.ch16

Guan, B., & Waliser, D. E. (2015). Detection of atmospheric rivers: Evaluation and application of an algorithm for global studies. *Journal of Geophysical Research: Atmospheres*, *120*(24), 12514–12535. https://doi.org/10.1002/2015JD024257

Guirguis, K., Gershunov, A., Hatchett, B., Shulgina, T., DeFlorio, M. J., Subramanian, A. C., et al. (2023a). Winter wet–dry weather patterns driving atmospheric rivers and Santa Ana winds provide evidence for increasing wildfire hazard in California. *Climate Dynamics*, *60*(5–6), 1729–1749. https://doi.org/10.1007/s00382-022-06361-7

Guirguis, K., Gershunov, A., Hatchett, B., Shulgina, T., DeFlorio, M. J., Subramanian, A. C., et al. (2023b). Catalog of winter weather patterns impacting California [Dataset]. *UC San Diego Library Digital Collections*. https://doi.org/10.6075/J089161B

Guirguis, K., Gershunov, A., Hatchett, B. J., DeFlorio, M. J., Subramanian, A. C., Clemesha, R., et al. (2023c). Subseasonal prediction of impactful California winter weather in a hybrid dynamical-statistical framework. *Geophysical Research Letters*, *50*(23), e2023GL105360. https://doi.org/10.1029/2023GL105360

Guirguis, K., Gershunov, A., Shulgina, T., Clemesha, R. E. S., & Ralph, F. M. (2019). Atmospheric rivers impacting Northern California and their modulation by a variable climate. *Climate Dynamics*, *52*(11), 6569–6583. https://doi.org/10.1007/s00382-018-4532-5

Haleakala, K., Brandt, T. W., Hatchett, B. J., Li, D., Lettenmaier, D. P., & Gebremichael, M. (2023). Watershed memory amplified the Oroville rain-on-snow flood of February 2017. *PNAS Nexus*, *2*(1), pgac295. https://doi.org/10.1093/pnasnexus/pgac295

Hatchett, B. J., Daudert, B., Garner, C. B., Oakley, N. S., Putnam, A. E., & White, A. B. (2017). Winter snow level rise in the northern Sierra Nevada from 2008 to 2017. *Water*, *9*(11), 899. https://doi.org/10.3390/w9110899

Hatchett, B. J., Koshkin, A. L., Guirguis, K., Rittger, K., Nolin, A. W., Heggli, A., et al. (2023). Midwinter dry spells amplify post-fire snowpack decline. *Geophysical Research Letters*, *50*(3), e2022GL101235. https://doi.org/10.1029/2022gl101235

Hoell, A., Hoerling, M., Eischeid, J., Wolter, K., Dole, R., Perlwitz, J., et al. (2016). Does El Niño intensity matter for California precipitation? *Geophysical Research Letters*, *43*(2), 819–825. https://doi.org/10.1002/2015GL067102

Hoerling, M. P., Kumar, A., & Zhong, M. (1997). El Niño, La Niña, and the nonlinearity of their teleconnections. *Journal of Climate*, *10*(8), 1769–1786. https://doi.org/10.1175/1520-0442(1997)010<1769:ENOLNA>2.0.CO;2

Horel, J. D., & Wallace, J. M. (1981). Planetary-scale atmospheric phenomena associated with the southern oscillation. *Monthly Weather Review*, *109*(4), 813–829. https://doi.org/10.1175/1520-0493(1981)109<0813:PSAPAW>2.0.CO;2

Hu, H., Dominguez, F., Wang, Z., Lavers, D. A., Zhang, G., & Ralph, F. M. (2017). Linking atmospheric river hydrological impacts on the U.S. West Coast to Rossby wave breaking. *Journal of Climate*, *30*(9), 3381–3399. https://doi.org/10.1175/JCLI-D-16-0386.1

Jiang, X., Waliser, D. E., Gibson, P. B., Chen, G., & Guan, W. (2022). Why seasonal prediction of California winter precipitation is challenging. *Bulletin America Meteorology Social*, *103*(12), E2688–E2700. https://doi.org/10.1175/BAMS-D-21-0252.1

Kalnay, E., Kanamitsu, M., Kistler, R., Collins, W., Deaven, D., Gandin, L., et al. (1996). The NCEP/NCAR 40-year reanalysis project [Dataset]. *Bulletin of the American Meteorological Society*, *77*(3), 437–471. https://doi.org/10.1175/1520-0477(1996)077<0437:tnyrp>2.0.co;2

Kintisch, E. (2016). How a 'Godzilla' El Niño shook up weather forecasts. *Science*, *352*(6293), 1501–1502. https://doi.org/10.1126/science.352.6293.1501

Kumar, A., & Chen, M. (2017). What is the variability in US west coast winter precipitation during strong El Niño events? *Climate Dynamics*, *49*(7–8), 2789–2802. https://doi.org/10.1007/s00382-016-3485-9

Leanard, A. (2023). Low-elevation snow, blizzard conditions in California amid season's coldest storm. *Washington Post*. Retrieved from https://www.washingtonpost.com/weather/2023/02/25/california-storm-los-angeles-blizzard-snow/

Liu, Y., Di, P., Chen, S., & DaMassa, J. (2018). Relationships of rainy season precipitation and temperature to climate indices in California: Long-term variability and extreme events. *Journal of Climate*, *31*(5), 1921–1942. https://doi.org/10.1175/JCLI-D-17-0376.1

Michaelis, A. C., Gershunov, A., Weyant, A., Fish, M. A., Shulgina, T., & Ralph, F. M. (2022). Atmospheric river precipitation enhanced by climate change: A case study of the storm that contributed to California's Oroville Dam crisis. *Earth's Future*, *10*(3), e2021EF002537. https://doi.org/10.1029/2021EF002537

National Weather Service. (2024). What is the Coop program? [Dataset]. Retrieved from http://www.nws.noaa.gov/om/coop/what-is-coop.html

Neiman, P. J., Ralph, F. M., Wick, G. A., Lundquist, J. D., & Dettinger, M. D. (2008). Meteorological characteristics and overland precipitation impacts of atmospheric rivers affecting the West Coast of North America based on eight years of SSM/I satellite observations. *Journal of Hydrometeorology*, *9*(1), 22–47. https://doi.org/10.1175/2007JHM855.1

O'Hara, B. F., Kaplan, M. L., & Underwood, S. J. (2009). Synoptic climatological analyses of extreme snowfalls in the Sierra Nevada. *Weather and Forecasting*, *24*(6), 1610–1624. https://doi.org/10.1175/2009waf2222249.1

Paek, H., Yu, J. Y., & Qian, C. (2017). Why were the 2015/2016 and 1997/1998 extreme El Niños different? *Geophysical Research Letters*, *44*(4), 1848–1856. https://doi.org/10.1002/2016GL071515

Patricola, C. M., O'Brien, J. P., Risser, M. D., Rhoades, A. M., O'Brien, T. A., Ullrich, P. A., et al. (2020). Maximizing ENSO as a source of western US hydroclimate predictability [Dataset]. *Climate Dynamics*, *54*(1–2), 351–372. https://doi.org/10.1007/s00382-019-05004-8

Ralph, F. M., Rutz, J. J., Cordeira, J. M., Dettinger, M., Anderson, M., Reynolds, D., et al. (2019). A scale to characterize the strength and impacts of atmospheric rivers. *Bulletin of the American Meteorological Society*, *100*(2), 269–289. https://doi.org/10.1175/bams-d-18-0023.1

Rasmusson, E. M., & Wallace, J. M. (1983). Meteorological aspects of the El Niño/Southern Oscillation. *Science*, *222*(4629), 1195–1202. https://doi.org/10.1126/science.222.4629.1195

Redmond, K. T., & Koch, R. W. (1991). Surface climate and streamflow variability in the western United States and their relationship to large-scale circulation indices. *Water Resources Research*, *27*(9), 2381–2399. https://doi.org/10.1029/91wr00690

Rhoades, A. M., Zarzycki, C. M., Inda-Diaz, H. A., Ombadi, M., Pasquier, U., Srivastava, A., et al. (2023). Recreating the California New Year's flood event of 1997 in a regionally refined Earth system model. *Journal of Advances in Modeling Earth Systems*, *15*(10), e2023MS003793. https://doi.org/10.1029/2023MS003793

Shulgina, T., Gershunov, A., Hatchett, B. J., Guirguis, K., Subramanian, A. C., Margulis, S. A., et al. (2023). Observed and projected changes in snow accumulation and snowline in California's snowy mountains. *Climate Dynamics*, *61*(9–10), 4809–4824. https://doi.org/10.1007/s00382-023-06776-w

Siirila-Woodburn, E. R., Dennedy-Frank, P. J., Rhoades, A., Vahmani, P., Maina, F., Hatchett, B., et al. (2023). The role of atmospheric rivers on groundwater: Lessons learned from an extreme wet year. *Water Resources Research*, *59*(6), e2022WR033061. https://doi.org/10.1029/2022WR033061

Wang, J., DeFlorio, M., Gershunov, A., Guirguis, K., Delle Monache, L., & Ralph, F. M. (2024). Modulation of western U.S. compound precipitation and temperature extremes by compounding MJO and ENSO interaction. *Communications Earth & Environment*, *5*(1), 314. in press. https://doi.org/10.1038/s43247-024-01449-w

Weaver, R. L. (1962). *Meteorology of hydrologically critical storms in California (No. 37)*. US Department of Commerce, Weather Bureau.

Zhang, T., Hoerling, M. P., Wolter, K., Eischeid, J., Cheng, L., Hoell, A., et al. (2018). Predictability and prediction of southern California rains during strong El Niño events: A focus on the failed 2016 winter rains. *Journal of Climate*, *31*(2), 555–574. https://doi.org/10.1175/JCLI-D-17-0396.1

References From the Supporting Information

Barnston, A. G., & Livezey, R. E. (1987). Classification, seasonality and persistence of low-frequency atmospheric circulation patterns. *Monthly Weather Review*, *115*, 1083–1126. https://doi.org/10.1175/1520-0493(1987)115%3C1083:CSAPOL%3E2.0.CO;2

Feldstein, S. B. (2000). The timescale, power spectra, and climate noise properties of teleconnection patterns. *Journal of Climate*, *13*(24), 4430–4440. https://doi.org/10.1175/1520-0442(2000)013<4430:TTPSAC>2.0.CO;2

Guirguis, K., Gershunov, A., Clemesha, R. E. S., Shulgina, T., Subramanian, A. C., & Ralph, F. M. (2018). Circulation drivers of atmospheric rivers at the North American West Coast. *Geophysical Research Letters*, *45*(22), 12576–12584. https://doi.org/10.1029/2018GL079249

Guirguis, K., Gershunov, A., DeFlorio, M. J., Shulgina, T., Delle Monache, L., Subramanian, A. C., et al. (2020). Four North Pacific atmospheric circulation regimes and their relationship to California precipitation on daily to seasonal timescales. *Geophysical Research Letters*, *47*(16), e2020GL087609. https://doi.org/10.1029/2020GL087609